Journal of Solid State Chemistry **148,** 229–235 (1999)
Article ID jssc.1999.8437, available online at http://www.idealibrary.com on IDEAL®

Synthesis and Characterization of H-*Ln*BO_3 Orthoborates (*Ln* = La, Nd, Sm, and Eu)

S. Lemanceau,* G. Bertrand-Chadeyron,* R. Mahiou,*,[1] M. El-Ghozzi,* J. C. Cousseins,* P. Conflant,† and R. N. Vannier†

*Laboratoire des Matériaux Inorganiques, Université Blaise-Pascal et ENSCCF, F-63177 Aubière Cedex, France; and
†Laboratoire de Cristallochimie et Physicochimie du Solide et ENSCL, F-59652 Villeneuve d'Ascq Cedex, France

Received February 19, 1999; in revised form June 2, 1999; accepted June 29, 1999

Depending on the ionic radius of the rare earth ions, orthoborates exhibit three different crystalline forms noted *Ln*BO_3 and H-*Ln*BO_3. A comparative study of the stability relationship of H-*Ln*BO_3 borate (*Ln* = La, Nd, Sm, and Eu) versus the temperature and synthesis method (solid state reaction and wet process) is reported. These high temperature forms have been characterized by X-ray diffraction, high temperature X-ray diffraction, and IR spectroscopy. This work was completed by a study of luminescence properties of H-$LaBO_3$ orthoborate doped by Eu^{3+}.

Key Words: **H-*Ln*BO_3; orthoborates; rare earths; synthesis; HTXRD; europium; luminescence.**

INTRODUCTION

In the course of the analysis of the relationship between the luminescence and the structure description of some rare earth-activated orthoborates corresponding to the empirical formula *Ln*BO_3 (*Ln* = La, Nd, Sm, and Eu), we have reinvestigated the domain of stability for these orthoborates using either conventional solid state reaction (SR) or wet processes (WP) to synthesize the compounds. The latter method (WP) has appeared to be very efficient to prepare high temperature phases (H-forms) at temperatures much lower than the ones used for the SR-route.

In 1961 Levin *et al.* (1) reported on the region of stability of the different structures in relation to borates' preparation temperature and ionic radius of the rare earth ions. He showed that the rare earth orthoborates *Ln*BO_3 present three crystallines of the $CaCO_3$ form, aragonite, vaterite, and calcite, which are dependent on the ionic radius of the rare earth. The compounds $LaBO_3$ and $NdBO_3$ exhibit the aragonite structure up to 1488 and 1090°C, respectively. $SmBO_3$ adopts the vaterite-type structure between 1050 and 1285°C. This structure is observed for $EuBO_3$ above 840°C. Two different forms denoted H-$LaBO_3$ and H-$NdBO_3$ have been found for La, Nd, and Sm at temperature above 1488, 1090, and 1285°C, respectively. Neodymium, samarium, and europium borates yielded high temperature forms similar to each other but different from lanthanum borate. According to Böhlhoff *et al.* (2), H-$LaBO_3$ crystallizes in the monoclinic system with $P2_1/m$ as the space group showing unique C_s point symmetry for the rare earth, whereas H-$NdBO_3$ type is triclinic with $P1$ as the space group. In this description the trivalent cations occupy four crystallographically nonequivalent sites (3).

The aim of this work is to study the stability relationships of H-*Ln*BO_3 borate (*Ln* = La, Nd, Sm, and Eu) versus the temperature and synthesis method (SR and WP routes). X-ray diffraction (XRD) and high temperature XRD (HTXRD) in the case of WP samples have been used to identify the several phases and their domains of stability depending on temperature. Infrared (IR) spectroscopy was used as complementary method in the identification of these compounds.

Relatively little is known about the optical properties of these compounds. Detailed investigation of the luminescence features of Eu^{3+} doped H-$LaBO_3$ has been undertaken.

EXPERIMENTAL RESULTS AND DISCUSSION

Techniques

Polycrystalline samples of *Ln*BO_3 and H-*Ln*BO_3 powder were characterized by X-ray powder diffraction. XRD patterns were obtained at room temperature by means of the DATA MP-Siemens D501 diffractometer and HTXRD patterns by a Guinier Lenné focusing camera.

The IR absorption spectra of the different samples in the powder form were recorded on the FTIR spectrophotometer, Nicolet type 5 SXC, transformed in the 400

[1]To whom correspondence should be addressed. Fax: +33 (0) 4 73 40 71 08; E-mail: mahiou@chimtp.univ-bpclermont.fr.

0022-4596/99 $30.00

and 4000 cm^{-1} frequency range. DTA and TG analysis was performed on a SETARAM thermogravimetric analyser. Xerogel samples were heated in air at a heating rate of 5°C min^{-1} for all data collection.

Luminescence measurements were performed between 14 and 300 K on H-$LaBO_3$: 5% Eu prepared by the WP method. The spectra were obtained with a tunable dye laser operated with rhodamine 590 or LDS 698 pumped by a frequency doubled Nd : YAG laser. For excitation in the $^5D_1$ and $^5D_2$ levels of Eu^{3+}, the output wavelength of the dye laser was shifted up by a quantum of 4155 cm^{-1} by stimulated Raman scattering in a high pressure gaseous H_2 cell. Excitation and emission spectra were recorded as previously described (4).

Synthesis

Powder samples of $LnBO_3$ and H-$LnBO_3$ were first obtained by direct reaction (SR) between boric acid (H_3BO_3) and the respective metal oxide. The reactants were weighed, finely ground, and mixed. The mixture was then transferred in a platinum crucible and heated in a furnace.

The samples were also prepared using the WP method. Starting materials were $Ln(NO_3)_3$, $6H_2O$ (0.2 M), H_3BO_3 (0.2 M) solutions and a 20% ammonia solution. The details of this method are described in Ref. (5). Different pH of synthesis was studied. Pure H-$LnBO_3$ phases were obtained with a pH 8 for Ln = La, Nd, and Sm, and pH 7 for Ln = Eu.

X-Ray Powder Diffraction

Analysis of the room temperature XRD powder patterns were carried out for $LnBO_3$ samples prepared by SR and WP methods. The relationship as stability of $LnBO_3$ orthoborates versus the temperature and synthesis method were established by recording the room temperature XRD spectra after heating the samples for 4 h at a given temperature. For each batch of the *Ln* rare earth compounds several samples were taken. The heating temperature for each sample of the same batch varied by 100°C. The derived results are collected in Tables 1 and 2 for the SR and WP samples, respectively. From these tables it appears clearly that the preparation mode influences considerably the composition and the purity of the phases.

Solid state reaction. For neodymium samples, above 1300°C was the high temperature form that H-$NdBO_3$ observed, whereas for La and Sm cations the high form had not yet appeared. Figure 1a shows the XRD pattern of this high form. This phase exists also at a low temperature but does not appear single phased. For lanthanum, samarium, and europium borates, H-forms were not observed at high temperatures. However, the XRD powder patterns for $LaBO_3$ below 750°C show clearly the simultaneous presence of H-$LaBO_3$, $LaBO_3$, and La_2O_3 phases in the sample.

TABLE 1
Stability Relationships of the $LnBO_3$-type Borates Prepared by Solid State Reaction as a Function of Temperature and Ionic Radius of the Rare Earth Ions

	500	600	700	750	800	900	1000	1100	1200	1300	θ°C
La	La_2O_3		$LaBO_3$ + La_2O_3 + H-$LaBO_3$		$LaBO_3$ (Aragonite)						
Nd	Nd_2O_3		$NdBO_3$ + Nd_2O_3 + H-$NdBO_3$		$NdBO_3$ (Aragonite)				$NdBO_3$ + H-$NdBO_3$		H-$NdBO_3$
Sm	Sm_2O_3		$SmBO_3$ + Sm_2O_3		$SmBO_3$ (Vaterite)						
Eu	Eu_2O_3		$EuBO_3$ + Eu_2O_3		$EuBO_3$ (Vaterite)						

Wet process. The stability diagram of the $LnBO_3$-type borate is very different for samples prepared by the wet process (Table 2) compared to the one obtained by solid state reaction. Indeed, at a low temperature pure H-$LnBO_3$ phases were observed for samples studied with Ln = La and Nd. The XRD patterns of H-$NdBO_3$ and H-$LaBO_3$ are presented in Figs. 1b and 2, respectively. $LaBO_3$ and $NdBO_3$ borates transform into the high forms (Table 2) at 500 and 600°C, respectively. Above 650 and 800°C lanthanum and neodymium borates exhibit the aragonite-type structure. However, neodymium borate showed a reversible

TABLE 2
Stability Relationships of the $LnBO_3$-type Borates Prepared by the Wet Process as a Function of Temperature and Ionic Radius of the Rare Earth Ions

	500	600	650	700	800	900	1000	1100	1200	1300	θ°C
La	Amorphous	H-$LaBO_3$			$LaBO_3$ (Aragonite)					H-$LaBO_3$	
Nd	Amorphous	H-$NdBO_3$		H-$NdBO_3$ + $NdBO_3$	$NdBO_3$ (Aragonite)				H-$NdBO_3$		
Sm	Amorphous	H-$SmBO_3$ + ε $SmBO_3$			H-$SmBO_3$ + $SmBO_3$ (Vaterite)			$SmBO_3$ (Vaterite)		H-$SmBO_3$	
Eu	Amorphous	H-$EuBO_3$ + ε $EuBO_3$			$EuBO_3$ (Vaterite)						

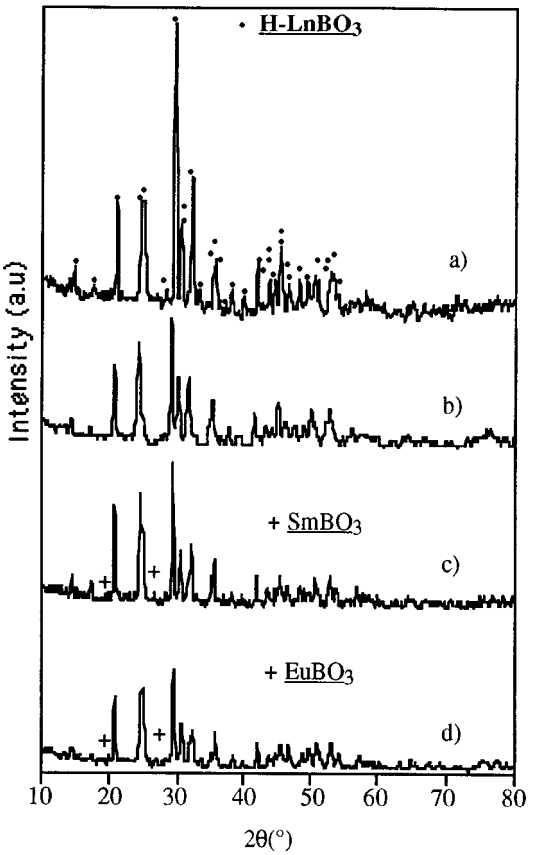

FIG. 1. XRD powder pattern of (a) H-$NdBO_3$ (1300°C) phase prepared by solid state reaction and (b) H-$NdBO_3$ (670°C), (c) H-$SmBO_3$ (720°C), and (d) H-$EuBO_3$ (700°C) phases prepared by the wet process.

transformation at 1200°C from the aragonite form to the high temperature form (H-$NdBO_3$). Samarium borate showed the high form above 1300°C and below 1100°C.

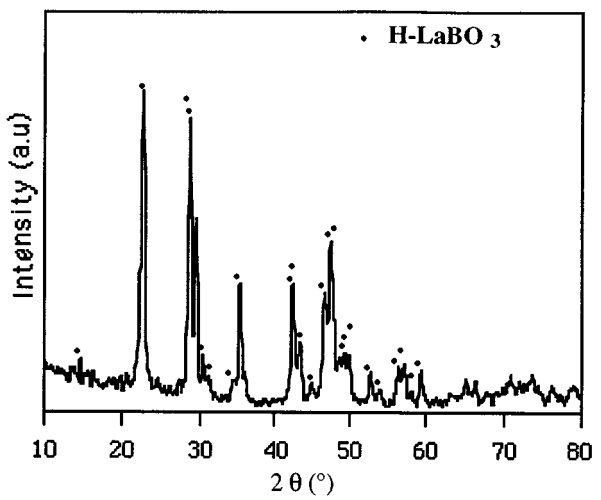

FIG. 2. XRD powder pattern of H-$LaBO_3$ (600°C) prepared by the wet process.

TABLE 3
Analysis of HTXRD Patterns Corresponding to $LnBO_3$ Powder Prepared by the Wet Process

	500	600 650	700	800 850	900
La	Amorphous	H-$LaBO_3$		$LaBO_3$ (Aragonite)	
Nd	Amorphous	H-$NdBO_3$		H-$NdBO_3$ + $NdBO_3$ (Aragonite)	
Sm	Amorphous	H-$SmBO_3$			
Eu	Amorphous	H-$EuBO_3$			

Between these two temperatures a vaterite-type structure is observed. However, the high temperature forms of $SmBO_3$ and $EuBO_3$ were never obtained in a pure form at a low temperature. As a matter of a fact, $SmBO_3$ and $EuBO_3$ vaterite types were present in minor amounts as a parasitic phase in the H-form (Figs. 1c and 1d). To confirm the above observation and to avoid any mistake which can be introduced by the heat treatment, for example, the samples have been checked by heating continuously between 100 to 900°C and recording the XRD patterns (XTXRD) at several points. The corresponding results collected in Table 3 agree with those of Table 2. The small differences observed in the temperature limits (around 50°C) are ascribed to a thermal kinetic effect. Probably, the $SmBO_3$ and $EuBO_3$ impurities are present with the high temperature forms on the Guiner–Lenné photographs; however, it is difficult to observe clearly their contributions.

Infrared Spectroscopy

IR spectroscopy was carried out with the objective of specifying and comparing the coordination of boron in $LnBO_3$ and H-$LnBO_3$ borates. Figure 3 presents the infrared spectra for the H-$LaBO_3$ and N-$NdBO_3$ WP samples. The observed vibration frequencies are listed in Table 4.

H-$LnBO_3$ forms with Ln = Nd, Sm, and Eu showed similar IR spectra. Both H-$LaBO_3$ and H-$LnBO_3$ (Ln = Nd, Sm, and Eu) borates have vibration modes which can be described as follows: ν_3 (asymmetric stretching) in the region 1100 and 1400 cm^{-1}, ν_1 (symmetric stretching) near 940 cm^{-1}, ν_2 (out of plane bending) in the region 700–800 cm^{-1}, and ν_4 (in-plane bending) below 670 cm^{-1}.

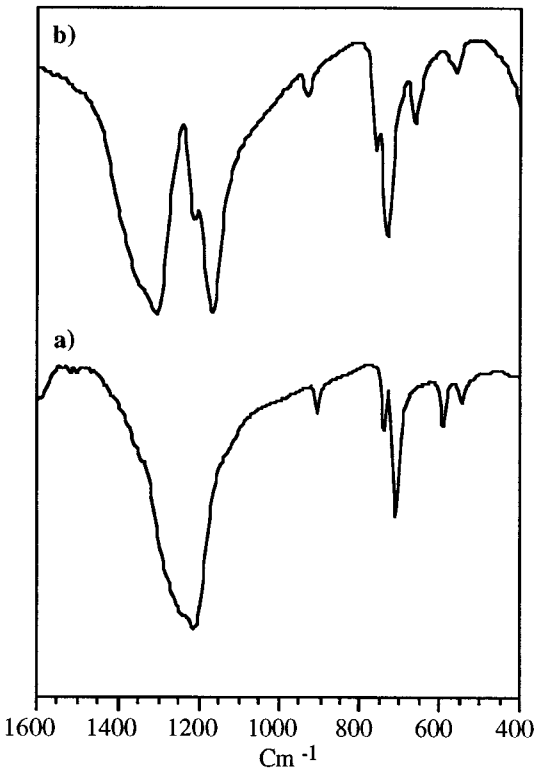

FIG. 3. Infrared spectra of (a) H-$LaBO_3$ and (b) H-$NdBO_3$ prepared by the wet process.

The close similarities in the IR spectra are evident. It will be noted that the behavior of v_3 in the two structures serves as a distinguishing feature. Indeed, four components of v_3 are observed for H-$NdBO_3$ while only two appear on the IR spectrum of the H-$LaBO_3$ phase (Fig. 3a).

For all these compounds it is clear that boron atoms are in threefold coordination. The observed frequencies between the 1350 and 1150 cm^{-1} range correspond to the stretching frequencies of a coordinated BO_3 group (6–9).

The structure of H-$NdBO_3$ consists of BO_3^{3-} anions and Nd^{3+} cations. The BO_3^{3-} anions are in the form of equilateral triangles with boron in the center. In this description (3), four types of BO_3 groups have been identified with B–O distances slightly different. Then, only one BO_3 group exists in the H-$LaBO_3$ structure (2).

The difference observed on the IR spectra concerning stretching vibrations of the B–O group in H-$NdBO_3$ and H-$LaBO_3$ phases may be explained by the fact that the number of anionic environments is different in the two structures.

Differential Thermal Analysis (DTA)

DTA curves realized for the xerogel are presented in Fig. 4 for H-$LnBO_3$ (*Ln* = La, Nd, Sm, and Eu).

Exothermic reaction peaks are observed for all compounds. These exothermics peaks are considered to be the result of the rapid evolution of heat caused by the formation of the respective phases $LnBO_3$ and H-$LnBO_3$ (10).

The X-ray diffraction patterns of the samples at the end of the heating curve (1100°C) and at the end of the cooling curve are identical. For lanthanum and neodynium compounds an aragonite structure is observed. The samarium sample shows the high temperature form and the europium sample shows the vaterite form.

TABLE 4
Observed Frequencies of the Different Vibration Modes in the $LnBO_3$ and H-$LnBO_3$ (*Ln* = La, Nd, Sm, Eu) Phases Prepared by the Wet Process

	$LaBO_3$, $NdBO_3$ aragonite (5–8)	$SmBO_3$, $EuBO_3$ vaterite (5–8)	H-$LaBO_3$ (600°C)	H-$LnBO_3$ (*Ln* = Nd 670°C, Sm 720°C, Eu 700°C)
Stretching vibrations of the B–O group in BO_3 (v_3 asymmetric stretching, v_1 symmetric stretching)	1273 v_3		1293 v_3	1347 v_3
	1089 v_3		1253 v_3	1307 v_3
				1200 v_3
		1051		1160 v_3
		1011		
	938 v_1	919	940 v_1	933 v_1
		871		
		844		
Deformation vibrations of the B–O group in BO_3 (v_2 out-of-plane bending, v_4 in-plane bending)	793 v_2		780 v_2	760 v_2
			753 v_2	
	712 v_2	709		720 v_2
	607 v_4		627 v_4	653 v_4
	585 v_4		580 v_4	580 v_4
		569		560 v_4
	529			

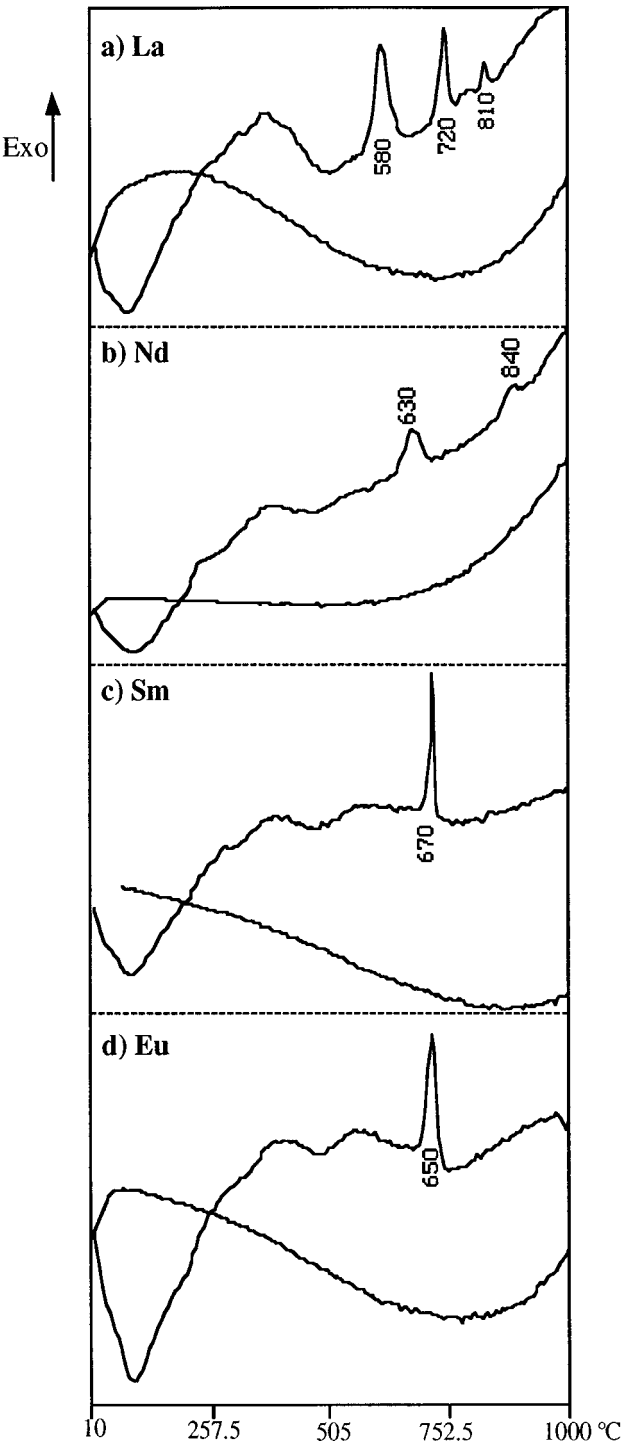

FIG. 4. DTA curves (heating and cooling) for H-$LnBO_3$ (Ln = La, Nd, Sm, and Eu).

The DTA curves of $SmBO_3$ and $EuBO_3$ present a similar behavior; indeed, an exothermic reaction peak corresponding to the formation of the high temperature form is observed at 670 and 680°C, respectively, for Sm and Eu (Figs. 4c and 4d). This result is in good agreement with the DXHT analysis.

For the lanthanum compound, three peaks appear (Fig. 4a), the first one at 580°C corresponds to the formation of the high temperature form. The second one at 720°C can be attributed to the transformation of the H-$LaBO_3$ phase to the aragonite phase. The peak at 810°C in Fig. 4a cannot be attributed to a phase transition. This is well confirmed by XRD and DXHT since no phase transition is observed for this temperature.

Figure 4b shows DTA of the neodynium compound. Two exothermic reaction peaks at 630 and 840°C, corresponding to the formation of the respective phases H-$NdBO_3$ and $NdBO_3$ aragonite, are identified.

Then a good correlation between DTA and DXHT results is observed for the borates studied.

Luminescence

The global time-resolved emission spectrum (TRS) shown in Fig. 5 was recorded at 14 K for a 5-mol% Eu^{3+} doped H-$LaBO_3$ sample under excitation in the $^5D_2$ level of Eu^{3+}. The three groups of narrow lines observed can be easily assigned to the $^5D_0 \rightarrow {}^7F_{0-2}$ transitions of the Eu^{3+} ion. The fact that only transitions from $^5D_0$ states are observed under blue $^7F_0 \rightarrow {}^5D_2$ excitation may be explained by the quenching of the emission from higher excited ^5D_J ($J = 1$–2) levels by efficient multiphonon de-excitation

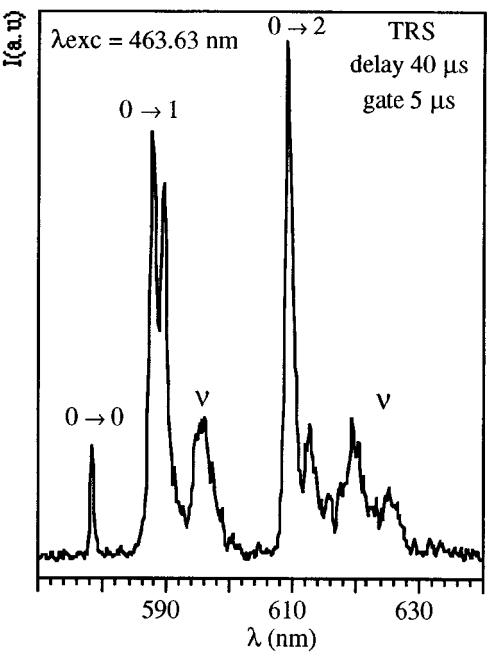

FIG. 5. Time-resolved emission spectrum of 5-mol% doped H-$LaBO_3$ at 14 K. The delay time after the laser pulse was 40 μs and the gate width was 5 μs.

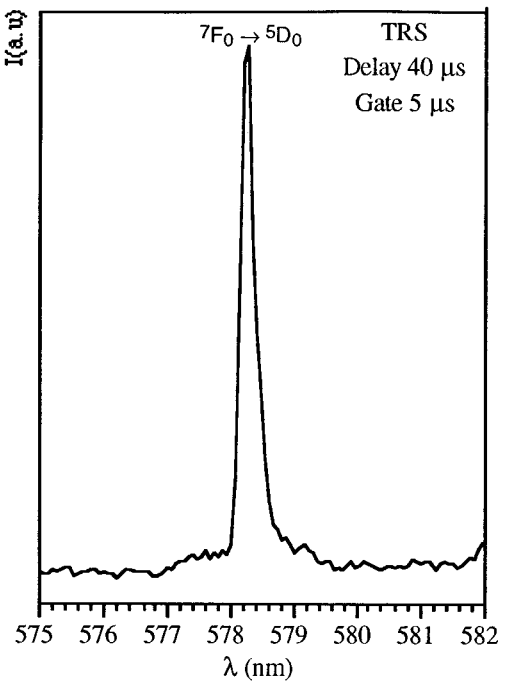

FIG. 6. $^7F_0 \rightarrow {}^5D_0$ excitation spectrum at 14 K obtained by monitoring the $^5D_0 \rightarrow {}^7F_1$ emission band for the 5-mol% Eu^{3+} doped H-$LaBO_3$.

processes associated with lattice vibrations. The vibronic coupling to the $^5D_0$ level seems to be rather strong since vibronic sidebands (v) are observed in the emission spectrum at the low energy scale of the $^5D_0 \rightarrow {}^7F_{1-2}$ transitions.

Figure 6 shows the $^7F_0 \rightarrow {}^5D_0$ TRS excitation spectrum obtained by monitoring the $^5D_0 \rightarrow {}^7F_1$ emission at 14 K. The spectrum consists of one peak located at 578.27 nm (Table 5). This result seems to indicate that the Eu^{3+} ions introduced into the matrix lie in one crystallographic site. To determine the symmetry of this site two excitation spectra have been recorded at 14 K in the spectral domain corresponding to $^7F_0 \rightarrow {}^5D_1$ and $^7F_0 \rightarrow {}^5D_2$ absorptions (Figs. 7a and 7b). The spectra consist for the $^7F_0 \rightarrow {}^5D_1$ and $^7F_0 \rightarrow {}^5D_2$ absorption, respectively, of 2 and 3 peaks. The positions of those are reported in Table 4.

Figures 8a and 8b present low temperature (14 K) $^5D_0 \rightarrow {}^7F_{1-2}$ emission spectra. The spectra exhibit two and three emission peak lines (Table 6) in agreement with the excitation spectra recorded for the same ΔJ ($\Delta J = 1, 2$).

The rare earth ions in the H-$LaBO_3$ structure occupy one crystallographic site of C_s symmetry following the structural

TABLE 5

Position of the $^7F_0 \rightarrow {}^5D_{0-2}$ Transitions Observed in the Excitation Spectra Obtained by Monitoring the $^5D_0 \rightarrow {}^7F_1$ Emission Bands for 5-mol% Eu^{3+} Doped H-$LaBO_3$ at 14 K

Transition	Wavelength (nm), (cm^{-1})
$^7F_0 \rightarrow {}^5D_0$	578.27 (17293)
$^7F_0 \rightarrow {}^5D_1$	525.26 (19038) 525.76 (19020)
$^7F_0 \rightarrow {}^5D_2$	463.63 (21569) 465.24 (21494) 465.90 (21464)

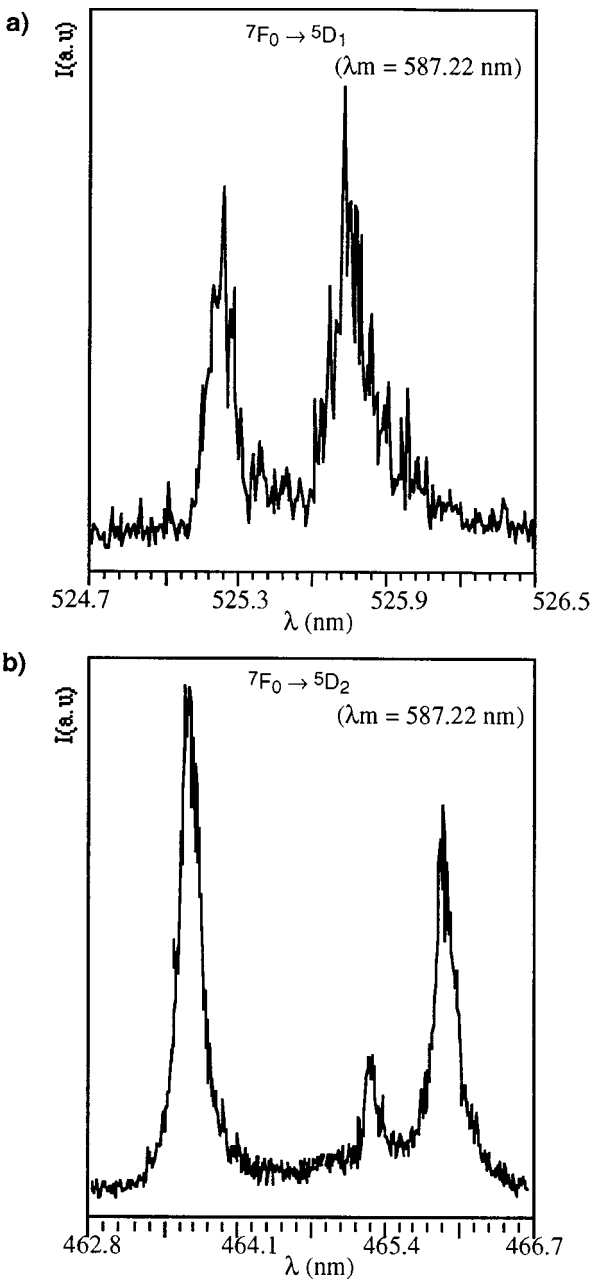

FIG. 7. (a) $^7F_0 \rightarrow {}^5D_1$ and (b) $^7F_0 \rightarrow {}^5D_2$ excitation spectra at 14 K obtained by monitoring the $^5D_0 \rightarrow {}^7F_1$ emission band for the 5-mol% Eu^{3+} doped H-$LaBO_3$.

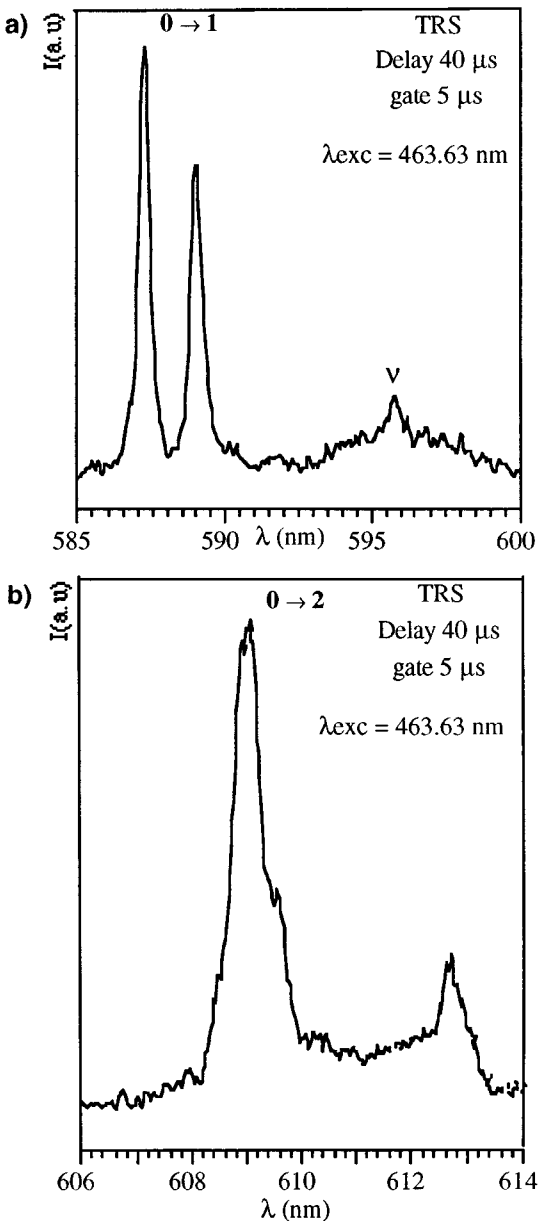

FIG. 8. (a) $^5D_0 \rightarrow {}^7F_1$ and (b) $^5D_0 \rightarrow {}^7F_2$ TRS emission spectra at 14 K for the 5-mol% doped H-$LaBO_3$.

description (2). The expected splitting for the J manifolds of Eu^{3+} ions in a C_s site are 1, 3, and 5 and for $J = 0$, 1, and 2, respectively.

The luminescence results indicate that the splitting for the J manifolds of Eu^{3+} ions in the H-$LaBO_3$ structure are 1, 2, and 3 for $J = 0$, 1, and 2, respectively. Hence, the observations

TABLE 6
Position of the $^5D_0 \rightarrow {}^7F_J$ ($J = 0-2$) Transitions of the 5-mol% Eu^{3+} Doped H-$LaBO_3$ Phase at 14 K

Transition	Wavelength (nm), (cm^{-1})
$^5D_0 \rightarrow {}^7F_0$	578.27 (17293)
$^5D_0 \rightarrow {}^7F_1$	587.22 (17029)
	588.97 (16979)
	609.07 (16418)
$^5D_0 \rightarrow {}^7F_2$	609.54 (16406)
	612.69 (16321)

do not agree with the structural data which indicates clearly that Eu^{3+} ion lies in a site of higher symmetry, probably, C_3 symmetry. To clarify this discrepancy the structural refinement of the H-$LnBO_3$ is in progress.

CONCLUSION

To conclude, synthesis by the wet process is an original route of preparation, which includes obtaining several high temperature forms of orthoborate H-$LnBO_3$ with *Ln* (La, Nd, Sm, and Eu) at low temperatures. Using XRD and HTXRD patterns has determined the temperature limits of the domain of stability for the H-phases.

Luminescence spectra indicate that the Eu^{3+} rare earth ion is distributed over one intrinsic crystallographic site. To keep the observed degeneracy of the $^7F_1$ and $^7F_2$ levels, the site symmetry group should have at least a C_3 axis. In order to confirm this result structural redetermination is undertaken from single crystals prepared by a flux evaporation process.

REFERENCES

1. E. M. Levin, R. S. Roth, and J. B. Martin, *Am. Miner.* **46,** 1030 (1961).
2. R. Böhlhoff, H. U. Bambauer, and W. Hoffman, *Z. Kristallogr.* **133,** 386 (1971).
3. K. K. Palkina, V. G. Kuznetsov, L. A. Butman, and B. F. Dzhurinskii, *Acad. Sci. URSS* **2,** 286 (1976).
4. G. Chadeyron, R. Mahiou, M. El-Ghozzi, A. Arbus, D. Zambon, and J. C. Cousseins, *J. Lumines*, **564,** 72 (1997).
5. G. Chadeyron, A. Arbus, M. T. Fournier, D. Zambon, and J. C. Cousseins, *C. R. Acad. Sci. Paris* **320,** 199 (1995).
6. J. P. Laperches and P. Tarte, *Spectrochim. Acta.* **22,** 1201 (1966).
7. C. E. Weir and R. A. Schroeder, *J. Res. Natl. Bur. Std. A* **68,** 465 (1964).
8. J. H. Denning and S. D. Ross, *Spectrochim. Acta. A* **28,** 1775 (1972).
9. V. I. Tsaryuk, V. D. Savchenko, V. F. Zolin, B. F. Dzhurinskii, G. V. Lysanova, and L. N. Margolin, *J. Appl. Spectr.* **59,** 895 (1993).
10. M. Sweeney, *Thermochim. Acta.* **11,** 397 (1975).